LAWRENCE
LIVERMORE
NATIONAL
LABORATORY

LLNL-TR-408754

Shock Properties of Fansteel85

D. J. Erskine, W. J. Nellis

November 17, 2008

Disclaimer

This document was prepared as an account of work sponsored by an agency of the United States government. Neither the United States government nor Lawrence Livermore National Security, LLC, nor any of their employees makes any warranty, expressed or implied, or assumes any legal liability or responsibility for the accuracy, completeness, or usefulness of any information, apparatus, product, or process disclosed, or represents that its use would not infringe privately owned rights. Reference herein to any specific commercial product, process, or service by trade name, trademark, manufacturer, or otherwise does not necessarily constitute or imply its endorsement, recommendation, or favoring by the United States government or Lawrence Livermore National Security, LLC. The views and opinions of authors expressed herein do not necessarily state or reflect those of the United States government or Lawrence Livermore National Security, LLC, and shall not be used for advertising or product endorsement purposes.

This work performed under the auspices of the U.S. Department of Energy by Lawrence Livermore National Laboratory under Contract DE-AC52-07NA27344.

Shock Properties of Fansteel85

David Erskine and William Nellis
Lawrence Livermore National Laboratory
P.O. Box 808 Livermore, CA 94550
Originally July 9, 1990, edited Sept. 16, 2008

The shock response of Fansteel85 was investigated in the pressure range 10-90 GPa. The linear U_s-U_p coefficients were found to be C=4.160±.015 km/s and S=1.195±.015. Ultrasound measurements yielded C_L=4.827 and C_T=2.101, implying a bulk sound speed C_B=4.173, which is in excellent agreement with the measured value for C. The Hugoniot elastic limit was determined to be 3.11±.05 GPa at U_p=.0595±.001 km/s and U_s=4.886±.01 km/s. The speed of sound in the material behind the shock front was determined to be 5.10±.06 km/s at 10.2 GPa and 5.25±.06 km/s at 20.6 GPa.

Fansteel85[1] is a high density (ρ =10.69 gm/cc) engineering alloy principally composed of tantalum and niobium (weight fractions 61% Nb, 28 %Ta, 10% W, 1% Zr). Its high density and strength make it an attractive construction material for example of shock recovery targets[2], where the kinetic energy of a projectile can be absorbed without serious distortion.

The shock behavior of Fansteel was investigated in the pressure range 10-90 GPa by electrical pin techniques and optical velocimetry. The shocks were generated by impact of flyer disks of aluminum or Lexan accelerated by a two-stage light gas gun in our laboratory. In this report, section I describes the results of shots where the shock transit time was measured by electrical shock-detecting pins. Details of the design of the target and data analysis for this experimental technique are described previously[3]. Section II describes the results and experimental technique for shots where optical velocimetry was used.

I. Electrical pin shots

With the electrical shock-detecting pin technique the target has the shape of a tophat, as shown in Fig. 1. Thirteen electrical shorting pins detect the passage of the shock through the planes of the "brim" of the hat, and at the top of the hat with a resolution of about 0.5 ns for each pin. The step height of the tophat is 2 mm. The six pins on the brim of the hat and the six at the top are called the *down* and *up* pins respectively. The XYZ location of the pins are determined to an accuracy of 1 μm in the Z-direction, and 0.1 mm in the XY plane. The location of the pins are such that they will

not be prematurely reached by side release waves. The design accommodates a 57° side release wave angle and the observed angle is calculated[4] to be 33°.

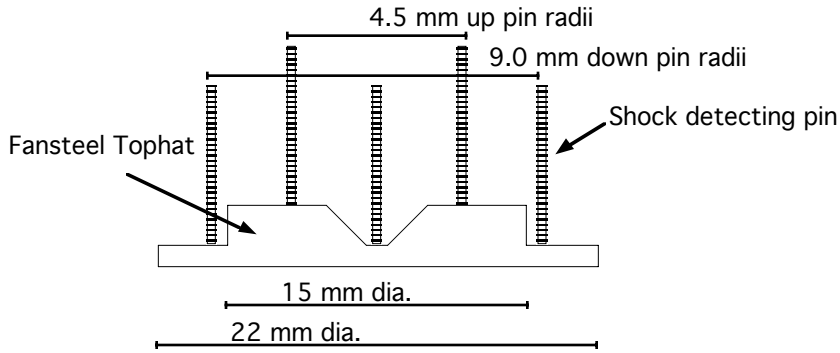

Figure. 1. Tophat target design for electrical pin determination of shock transit time. There are six *down* and six *up* pins. The center *bowing* pin is coplanar with the *down* pins and is used to determine the extent of curvature of the flyer plate, which impacts from below. The pins are spring loaded against the tophat.

The flyer disks were Aluminum 3 mm thick and 24 mm in diameter, supported by a Lexan sabot. The analysis assumes the shock front is primarily planar with a small parabolic component. A shorting pin (denoted the *bowing* pin) located at the center of the target on the lower plane allows a determination of the amount of bowing of the flyer disk (typically <2 ns). The data is analyzed by plotting the arrival times and locations in XY and t-space and fitting the data to two parallel planes, for the *down* and *up* pin groups. The separation between the best-fit planes is the transit time, with a correction[3] made for parabolic bowing.

The results of 3 pin shots are tabulated in Table I and plotted in Figure 2. In estimating the net uncertainty in U_s, we considered the scatter of arrival times about the best-fit planes, the uncertainty in pin locations and the tilt of the shock wave planes, and a 0.5 ns intrinsic uncertainty assigned to the bowing pin.

Table I. Summary of electrical pin shot results. Velocities are in km/s. Bowing is positive if bowing pin fires late. U_p is calculated by impedance matching using U_s and a standard aluminum Hugoniot.

Shot#	U_{flyer}	Us	Up	Bowing(ns)
p6	3.771	5.488±.014	1.104±.005	–0.9
p8	4.800	5.877±.01	1.439±.006	–1.3
p9	2.591	5.036±.002	0.735±.004	–0.9

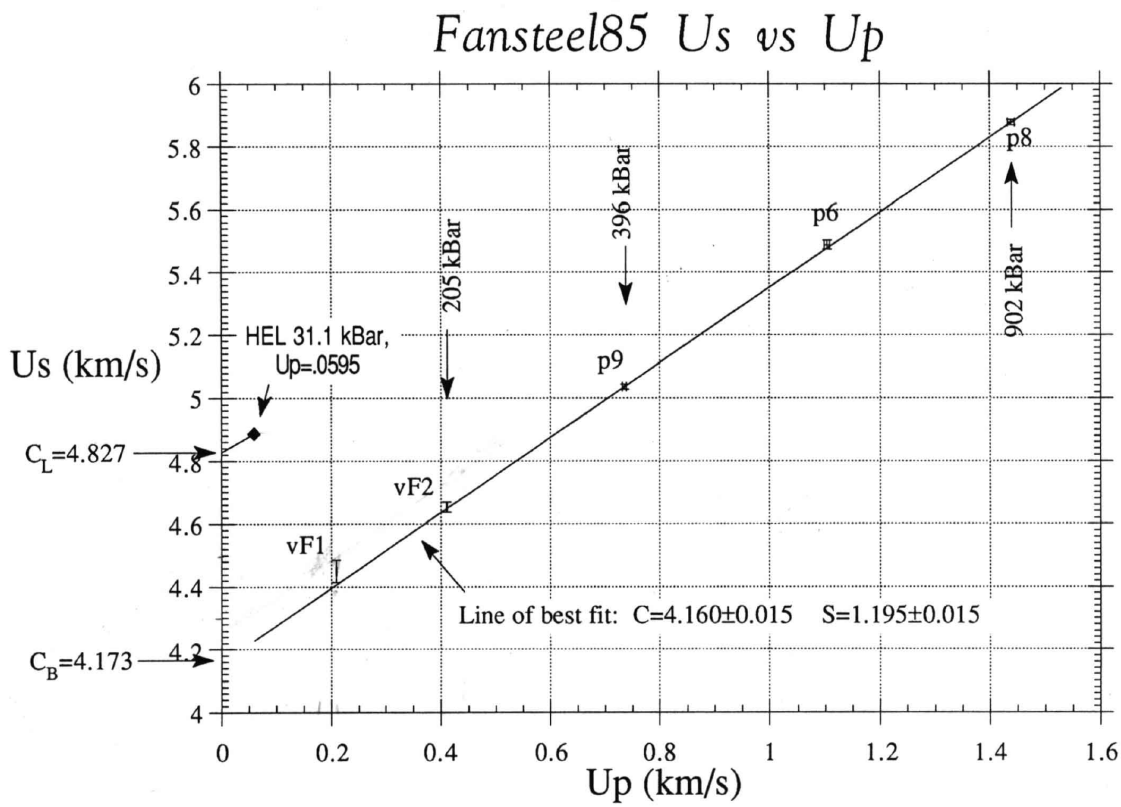

Figure 2. Us-Up results for the electrical shorting pin and velocimetry shots. A weighted least squares fit to shots p6, p8, p9 and vF2 yields the solid line with the stated coefficients. The computed bulk sound speed from the ultrasound measurements agrees closely with C of the best fit. Shot vF1 has a relatively larger uncertainty due to the extended risetime of the plastic wave. The diamond datum indicates the deduced Hugoniot elastic limit (HEL). The elastic speed at the HEL is 4.886 km/s.

II. Velocimetry Shots

Two shots were fired using a VISAR velocimeter[5] to measure the velocity history of the shock emerging from the rear of a Fansteel layer into a LiF window. The target design is shown in Fig. 3 and specified in Table II.

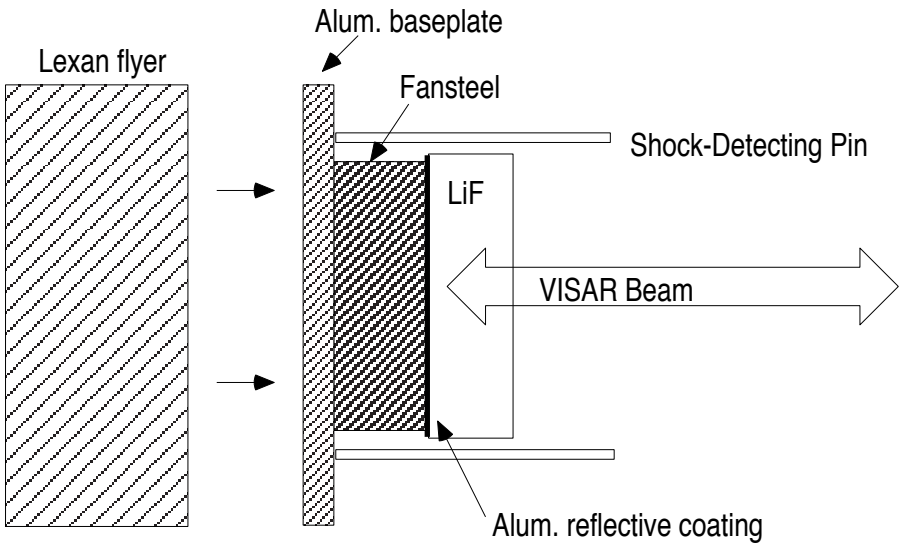

Figure. 3. Target design for VISAR velocimetry. There are six *down* shock-detecting pins. A thin aluminum coating on the LiF window at the Fansteel interface reflects the VISAR laser beam. Movement of the interface Doppler shifts the reflected light, encoding it with velocity information resolved by the VISAR interferometer.

Table II. Velocimetry target specifications. Dimensions in mm.

	targets vF1 &vF2	vF2, if different from vF1
6061 ALUM. BASEPLATE		
thickness	1.497	1.481
density	2.7005	
FANSTEEL		
thickness	5.484	
diameter	14.4	
density	10.692	
LiF WINDOW		
thickness	4.772	4.776
diameter	15	
density	2.649	

A. How it Works

The velocimeter works by detecting the Doppler shift imparted to a laser beam reflecting off the moving surface of the target. An interferometer converts the wavelength shifts into optical fringes, which are in turn detected by photomultipliers. The electrical signals are later analyzed into velocity information. The resolution of our VISAR is 1 ns and 0.5 m/s.

The light is reflected off a thin aluminum coating applied to the LiF window surface at the Fansteel interface. Six electrical shock-detecting pins coplanar with the front surface of the Fansteel layer determine the start of the shock transit through the Fansteel. The end of the transit is detected optically by the VISAR probe beam. The difference in arrival times between the electrical pins and the VISAR signal gives the shock transit time through the Fansteel layer, after fixed instrumental and cable delays between the electrical and optical systems have been accounted. This relative delay between the electrical and optical systems was measured (±1 ns) by separate experiments. The XY location of the electrical pins and the optical axis of the VISAR beam was measured accurately so that the effect of tilting of the shock plane on the transit time could be included.

Since a central bowing pin was not present, the amount of bowing of the Lexan flyers could not be determined and was assumed to be zero. This is a reasonable assumption, since the Lexan flyer is thicker than its diameter and the impact velocities were not high. In any case, the ~1 ns uncertainty this generates is insignificant compared to the uncertainty in the transit time due to the ill-defined edge of the shock (4 - 10 ns) discussed below.

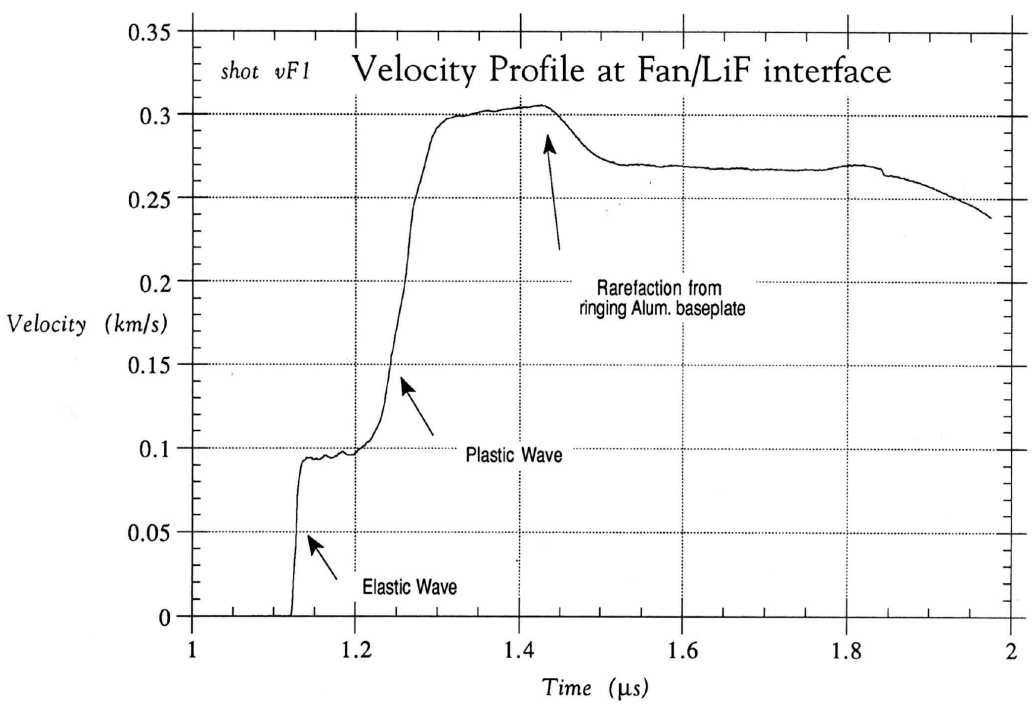

Figure 4. Velocity profile of shot *vF1* measured at the Fansteel/LiF interface. The horizontal axis is time after the shock has entered the Fansteel layer, as determined from the electrical pins. The downward step following the plastic wave is attributed to a rarefaction coming from a double transit of the shock through the aluminum baseplate after reflecting from the Fansteel layer.

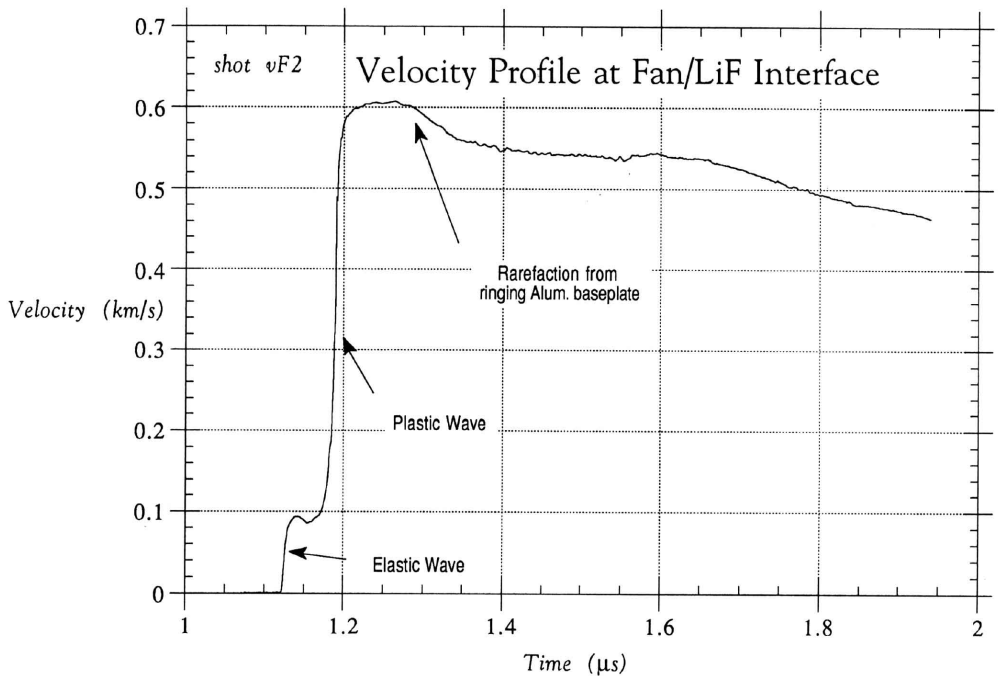

Figure 5. Velocity profile of shot *vF2*measured at the Fansteel/LiF interface. The character of the features have changed compared to shot *vF1* due to the increase intensity of the impact. The plastic wave and its effect on the rear of the window have sharpened, and the arrival time difference between elastic and plastic waves has narrowed.

B. The Data

The velocity profiles obtained from the two shots are shown in Figures 4 and 5. Although the elastic wave is clearly defined in both shots, the plastic waves have a relatively greater risetime. We took the difference in plastic and elastic arrival times to be 110±10 ns for shot *vF1* and 56±4 ns for shot *vF2*.

The downward step following the plastic wave is attributed to a rarefaction arising from a double transit of the shock across the aluminum baseplate after initially reflecting from the Fansteel layer. The periodic fine structure at the top of the elastic wave in *vF1* and *vF2* may be related to the finite rate of the elastic-to-plastic transformation.

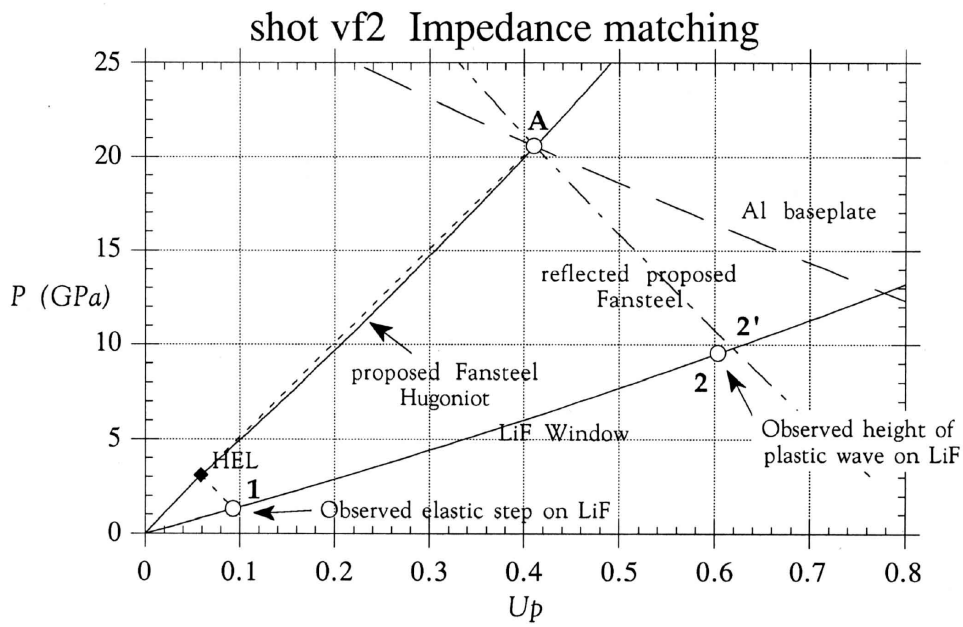

Figure 6. Impedance matching for shot *vf2*, to determine HEL, and U_p of the plastic wave. An HEL of 3.11 GPa is deduced from the observed elastic step height (pt. 1) and elastic wave speed (determining the slope from the origin to HEL). A dashed line extending from the HEL having a slope of $\rho U_s'$, where U_s' is determined from the plastic wave speed, intersects the aluminum baseplate reflected Hugoniot at point A, yielding U_p. The proposed Fansteel Hugoniot (from the best-fit of all the data) is also drawn for comparison. A reflection of the Fansteel Hugoniot about pt. A intersects the LiF Hugoniot at pt. 2', near the measured plastic wave height pt. 2. The discrepancy is most likely a hysteresis due to the strength of the material.

C. Impedance Matching

Figure 6 illustrates the impedance matching analysis used to calculate the Hugoniot elastic limit (HEL) and the U_s and U_p of the wave in the Fansteel. Using the LiF Hugoniot U_s=5.15+1.352U_p, and the relation $P=\rho U_s U_p$, the measured interface velocity profile can be converted to a pressure history at the Fansteel/LiF interface. The pressures at the window of the elastic and plastic parts of the profile, are listed in Table III as $P1_{LiF}$ and $P2_{LiF}$ respectively, and are plotted as points 1 and 2 in Fig. 6.

Table III. Data for impedance matching. $P1_{LiF}$ and $P2_{LiF}$ are the pressures on the LiF window of the elastic wave and plastic waves respectively, computed from measured particle velocities through the LiF Hugoniot. U_{elast} is the speed of the elastic wave in km/s, computed from the arrival time.

		ELASTIC		PLASTIC
Shot#	Flyer speed (km/s)	U_{elast}	$P1_{LiF}$(GPa)	$P2_{LiF}$(GPa)
vF1	1.666	4.888	1.32	4.4
vF2	2.761	4.884	1.30	9.5

1. Hugoniot Elastic Limit

From Table III it can be noted that $P1_{LiF}$ and U_{elast} are nearly the same for both shots *vF1* and *vF2*. We used the average of these values to calculate the HEL.

The elastic wave speed is modeled to change linearly from its ambient value of 4.827 (from the Appendix) to 4.886 at the HEL. By iteration, using the knowledge that a reflection of this elastic Hugoniot we are seeking should intersect the LiF Hugoniot at point 1, we find that

$$U_{elastic}=4.827 + 1.0U_p, \qquad (1)$$

and the HEL is at U_{pHEL}=.0595±.001 km/s, and P_{HEL}=3.11±.05 GPa, indicated by the diamond datum in Fig. 6.

2. Plastic Wave Us-Up

The shock speed of the plastic wave (U_s) is found from its arrival time, and the particle velocity of the Fansteel behind the plastic wave (U_p) is found by the impedance matching described below. In Fig. 6, an line (dashed) is drawn from the HEL datum having a slope $\rho_{HEL}U_s'$, where $Us'=U_s-U_{pHEL}$ and ρ_{HEL} is the density at HEL. The point of intersection of this line with the reflected Hugoniot of the aluminum baseplate yields U_p, indicated by the circular datum labeled "A". (The aluminum curve is determined from prior impedance matching with the Lexan Hugoniot, not shown).

The results of the impedance matching analysis for both shots are tabulated in Table IV. The two U_s-U_p velocimetry data are combined with the pin shot data in Figure 2 to yield a best fit line, which corresponds to the curve labeled "proposed Fansteel Hugoniot" in Fig. 6.

A consistency check on this result is provided by comparing the measured plastic wave height ($P2_{LiF}$, point 2) with that calculated from impedance matching (point 2'). The latter is found by reflecting the proposed Fansteel Hugoniot about point A and intersecting it with the LiF Hugoniot. We find that the experimental values are slightly less than calculated values (9.5 versus 9.8 GPa for shot *vF1*, and 4.4 versus 4.75 GPa for shot *vF2*). This slight hysteresis is likely a manifestation of the strength of the material, and can be expected for a material that follows the ideal elastic-plastic response[6].

Table V. Summary of velocimetry shot impedance matching results. U_s is determined from the arrival time. U_p is calculated by impedance matching using U_s and standard aluminum and Lexan Hugoniots. Velocities in km/s.

Shot#	Up	Us
vF1	0.2086±.004	4.450±.036
vF2	0.4108±.004	4.652±.016

III. RESULTS

A. Us-Up Relation

A weighted least-squares fit through the U_s-U_p data of Fig. 2, excluding the point with the greatest uncertainty, yields for Fansteel:

$$U_s = 4.160 + 1.195\ U_p \qquad (2)$$

in km/s. The velocimetry shot *vF1* has comparatively larger uncertainty than the other shots because of the finite risetime of the plastic wave.

The uncertainty (σ) of the fit for U_s varies with U_p and is a minimum in the vicinity of the cluster of data. If a quadratic expression is used to approximate the U_p dependance of 2σ as in

$$2\sigma = A_0 + A_1 U_p + A_2 U_p^2 \qquad (3)$$

then the coefficients are A_0=0.0351, A_1=–0.0494, and A_2=0.2524 with U_p in km/s.

The best fit value for C (4.160 km/s) agrees well with the bulk sound speed C_B=4.173 km/s, derived from the ultrasound data using the relation

$$C_B^2 = C_L^2 - \frac{4}{3} C_T^2 \qquad (4)$$

and C_L and C_T from Table V in the appendix.

B. Sound Speed

The speed of sound (*ss*) in the Fansteel behind the plastic wave can be estimated from the observed arrival time of the downturn in the velocity signal seen soon after the plastic wave. A hydrocode calculation[7] was used to calculate the double transit time of the shock in the aluminum baseplate. Movement of the front and rear Fansteel interfaces was considered in calculating the length of material transited. We obtain 5.10 ±0.06 km/s at 10.2 GPa and 5.25±0.06 km/s at 20.6 GPa for shots *vF1* and *vF2* respectively. These sound speeds are relative to the material velocity behind the shock.

Sound speeds calculated by McQueen's formula[8] based on the slope of the isentrope yield *ss*=4.43 and 4.68 km/s respectively for shots *vF1* and *vF2* when the Gruneisen parameter γ = 1.67. Our measured sound speeds our larger than these calculated values, most likely because the calculated values do not account for the finite strength of the material.

ACKNOWLEDGEMENTS

Thanks to Doug Ravizza for construction of the velocimetry targets and Larry Cassidy for the tophat targets. This work was performed under the auspices of the U. S.

Department of Energy by the Lawrence Livermore National Laboratory under Contract DE-AC52-07NA27344.

APPENDIX

Table V. Ultrasonic Characterization[9].

Geometry	Disk, 38 mm diameter
Thickness (mm)	2.7432
Density (gm/cc)	10.689
Frequency, MHz Vl	10
Frequency, MHz Vs	5
Longitudinal Velocity C_L (km/s)	4.82695
Shear Velocity C_T (km/s)	2.10051
The shear velocity was found to be slightly anisotropic (0.2% relative to listed average)	
Thin Rod Velocity	3.49367
Poisson's Ratio	0.3832
Young's Modulus (GPa)	130.47
Shear Modulus (GPa)	47.16
Lame Modulus (GPa)	154.72
Bulk Modulus (GPa)	186.16

References

1. Supplied by Jess West of Lawrence Livermore Nat. Lab.
2. W.J. Nellis, C.L. Seaman, M.B. Maple, E.A. Early, J.B. Holt, M. Kamegai, G.S. Smith, D.G. Hinks and D. Dabrowski, Lawrence Livermore Lab. Report UCRL-100472.
3. A.C. Mitchel and W. J. Nellis, Jrnl. Appl. Phys. **52**, 3363 (1981).
4. L.V. Al'tshuler, et al. Soviet Phys. JETP 11 766-775 (1960).
5. Our **V**elocity **I**nterferometer **S**ystem for **A**ny **R**eflector is similar in concept to that described by W. F. Hemsing, Rev. Sci. Instrum. 50, 73 (1979).
6. L. Davisson, R. A. Graham, Physics Reports 55, 292 (1979).
7. GEM computer code, G. Greeman, K. Hainebach, J. A. Leibee, C. Lund and J. Rogers, Lawrence Livermore Nat. Lab.
8. R. G. McQueen, S.P. Marsh, and J.N. Fritz, Jrnl. GeoPhys. Rsrch., 72, 4999 (1967), Equation 30.
9. Performed by Albert E. Brown, Lawrence Livermore Nat. Lab., 12/8/89.